Journal of Engineering Mathematics **46:** 313–330, 2003.

The BEM for plates of variable thickness on nonlinear biparametric elastic foundation. An analog equation solution

J.T. KATSIKADELIS and A.J. YIOTIS
School of Civil Engineering, National Technical University of Athens, Zografou Campus, GR-157 73 Athens, Greece

Received 31 May 2002; accepted in revised form 28 March 2003

Abstract. The BEM is developed for the analysis of plates with variable thickness resting on a nonlinear biparametric elastic foundation. The presented solution is achieved using the Analog Equation Method (AEM). According to the AEM the fourth-order partial differential equation with variable coefficients describing the response of the plate is converted to an equivalent linear problem for a plate with constant stiffness not resting on foundation and subjected only to an 'appropriate' fictitious load under the same boundary conditions. The fictitious load is established using a technique based on the BEM and the solution of the actual problem is obtained from the known integral representation of the solution of the substitute problem, which is derived using the static fundamental solution of the biharmonic equation. The method is boundary-only in the sense that the discretization and the integration are performed only on the boundary. To illustrate the method and its efficiency, plates of various shapes are analyzed with linear and quadratic plate thickness variation laws resting on a nonlinear biparametric elastic foundation.

Key words: analog equation, boundary elements, nonlinear foundation, plates, variable thickness

1. Introduction

The study of plates with variable thickness is pursued in various engineering disciplines, such as civil engineering, aerospace engineering and the design of machines. Although there is an extensive literature on plates with constant thickness, a rather limited amount of technical literature is available on the solution of problems dealing with plates of non-uniform thickness. The reason for this is that in the case of plates with variable thickness, the governing differential equation is found to have variable coefficients, and this fact increases the difficulty of the solution. Prior to the advent of computers, plates with variable thickness could be analyzed only for certain simple geometries, boundary conditions and thickness variation laws. The existing analytic solutions are limited to circular and annular plates with linear varying thickness along the radius subjected to axisymmetric loading, as well as to rectangular plates with unidirectional thickness variation amenable to use Levy-type solutions. Approximate methods, such as the Galerkin method and the Rayleigh- Ritz method, have also been used to treat this problem. Some papers by Katsikadelis and Nerantzaki [1–4] include literature surveys on plates with variable thickness analyzed by analytical and/or approximate methods; therefore no attempt to review the literature will be made here.

An arbitrary thickness profile can be treated only by numerical methods. The finite-difference method (FDM), the finite-element method (FEM) and the boundary-element method (BEM) are candidates to treat the problem at hand. Although the FDM can solve static problems for plates with variable thickness, its efficiency is drastically restricted when the geom-

etry of the plate and the boundary conditions are not simple. The FEM can adequately solve static and dynamic problems for plates with variable thickness. Certain commercial computer codes for structural analysis include plate elements with variable thickness. However, no publications have appeared using FEM when the subgrade reaction is taken into account. With regard to the BEM, although there is considerable application of this method to the analysis of plates with constant thickness (*e.g.* [5–9]), little work has been published on plates with variable thickness using the BEM. This is obviously because a fundamental solution for the governing equation cannot be established, at least in a form that could be useful to develop a pure boundary-element method. A first attempt to use BEM for plates with variable thickness has been made by Sapountzakis and Katsikadelis [10] and Katsikadelis and Sapountzakis [11], who employed the fundamental solution of the plate with constant thickness and treated the term involving derivatives up to the third order as an unknown field quantity. The use of a Gauss integration scheme on the whole domain of the plate proposed by these authors alleviated the method from discretizing the domain into cells. Thus, this method retained most of the advantages of a BEM solution over the pure domain-discretization method. Chaves *et al.* [12] presented an alternative BEM formulation for plates with variable thickness by taking an appropriate form of Betti's theorem to derive integral representations of displacements and internal forces. Recently, a more effective BEM-based method for the analysis of plates with variable thickness has been developed by Nerantzaki and Katsikadelis [1–4] using the concept of the analog equation introduced by Katsikadelis [13]. Though this method requires domain discretization to evaluate the domain integrals, it is more versatile and can treat the static and dynamic problem including also in-plane forces.

In this paper the AEM is further developed and applied to the problem at hand as a boundary-only method by converting the domain integrals containing the fictitious load to boundary ones. This is achieved by approximating the fictitious load with a radial basis function series. Thus, the method retains all the advantages of the pure BEM using a known simple fundamental solution, *i.e.*, that of the biharmonic equation and it is applied to the problem of plates with variable thickness resting on a nonlinear biparametric elastic foundation. The application of the method is illustrated by solving several example problems of plates with linear and quadratic thickness variation laws and resting on a linear or nonlinear biparametric elastic foundation. Since no numerical results are available in the literature for the studied problems, the accuracy of the results is validated by considering plates approaching the plate with constant thickness and resting on a linear elastic foundation.

2. Governing equation

Consider a thin elastic plate of variable thickness, $h = h(\mathbf{x})$, $\mathbf{x} : \{x, y\} \in \Omega$ occupying the two-dimensional multiply connected domain Ω of the x, y-plane, bounded by the $K + 1$ curves $\Gamma_0, \Gamma_1, \Gamma_2, \ldots, \Gamma_K$. The curves $\Gamma_i (i = 0, 1, 2, \ldots, K)$ may be piece-wise smooth (Figure 1). Assuming that there is no abrupt variation in thickness, the expressions for bending and twisting moments derived for plates of constant thickness apply with sufficient accuracy to this case also [14, pp. 173–174] and the equilibrium of a plate element subjected to a distributed transverse load $g(\mathbf{x})$, and subgrade reaction $p(w, \nabla^2 w)$ yields the following differential equation in terms of the deflection $w(\mathbf{x})$ in Ω

$$D\nabla^4 w + 2D_{,x}(\nabla^2 w)_{,x} + 2D_{,y}(\nabla^2 w)_{,y} + \nabla^2 D \nabla^2 w - (1-\nu)(D_{,xx} w_{,yy} - 2D_{,xy} w_{,xy} + D_{,yy} w_{,xx}) + p(w, w_{,x}, w_{,y}, w_{,xy}, \ldots, w_{,yyyy}) = g(\mathbf{x}), \tag{1}$$

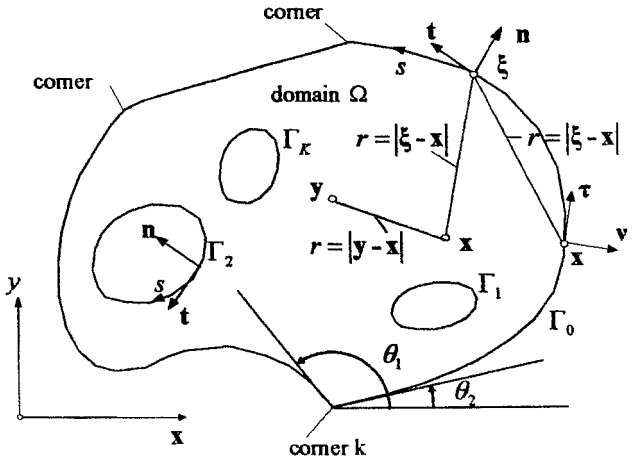

Figure 1. Plate geometry and notation.

where $D = Eh^3/12(1-\nu^2)$ is the variable flexural stiffness of the plate and $p(w, w_{,x}, w_{,y}, w_{,xy}, \ldots, w_{yyyy})$ is a nonlinear function of the deflection and its derivatives up to the fourth order representing the subgrade reaction. It should be noted, however, that usual realistic subgrade models depend mostly on the deflection and its Laplacian, *i.e.*, $p(w, \nabla^2 w)$, and, without restricting the generality, this is the model that will be used in our applications. Moreover, the deflection w must satisfy the following boundary conditions on the boundary $\Gamma = \bigcup_{i=0}^{i=k}$:

$$\alpha_1 w + \alpha_2 V^*(w) = \alpha_3, \qquad \beta_1 w_{,n} + \beta_2 M^*(w) = \beta_3, \tag{2a,b}$$

where $\alpha_i = \alpha_i(\mathbf{x})$, $\beta_i = \beta_i(\mathbf{x})$, $\mathbf{x} \in \Gamma$, are functions specified on Γ; $M^*(w)$ and $V^*(w)$ are the normal bending moment and the effective shear force on the boundary. The boundary conditions (2a,b) are the most general linear boundary conditions for the plate-bending problem, including also transverse and rotational elastic support. All types of conventional boundary conditions can be derived from (2a,b) by specifying appropriately the functions α_i and β_i.

Taking into account that the flexural rigidity D is a position-dependent function and using boundary curvilinear coordinates n and s, we may write the operators M^*, V^* appearing in Equations (2a,b)

$$M^* = -D[\nabla^2 + (\nu-1)(\frac{\partial^2}{\partial s^2} + \kappa\frac{\partial}{\partial n})], \tag{3a}$$

$$\begin{aligned} V^* = -D[\frac{\partial}{\partial n}\nabla^2 - \ (\nu-1)\frac{\partial}{\partial s}(\frac{\partial}{\partial n\partial s} - \kappa\frac{\partial}{\partial s})] + \frac{\partial D}{\partial s}(\nu-1)(\frac{\partial^2}{\partial n\partial s} - \kappa\frac{\partial}{\partial s}) \\ -\frac{\partial D}{\partial n}[\nabla^2 + (\nu-1)(\frac{\partial^2}{\partial} s^2 + \kappa\frac{\partial}{\partial n})], \end{aligned} \tag{3b}$$

in which $\kappa = \kappa(s)$ is the curvature of the boundary; $\partial/\partial s$ and $\partial/\partial n$ denote differentiation with respect to the arc length s of the boundary, and the outward normal n to it, respectively.

In the case of free or transversely elastically restrained edges, the boundary conditions (2a,b) must be supplemented with the corner condition

$$c_{1l} w + c_{2l} [\![T^*(w)]\!]_l = c_{3l}, \, c_{2l} \neq 0, \tag{4}$$

where c_{ik} are specified constants at the corner point $\mathbf{x}_l$ and T^* is the operator

$$T^* = D(1-\nu)\left(\frac{\partial^2}{\partial s \partial n} - \kappa \frac{\partial}{\partial s}\right). \tag{5}$$

Thus, $T^*(w)$ is the twisting moment along the boundary and $[\![T^*(w)]\!]_l$ is its jump of discontinuity at the corner point $\mathbf{x}_l$.

It should be emphasized that for the biparametric foundation the free boundary, in contrast to the clamped, allows interaction between the deflections of the foundation area under the plate and that of outside it. Therefore the boundary condition (2a) should be appropriately modified on the following physical considerations [15]:

a. The deflection is continuous across the boundary Γ, while its normal derivative is discontinuous;
b. The bending moment $M^*(w)$ vanishes on Γ;
c. The jump of the shear force in the shear layer on Γ is equal to the effective shear force of the plate $V^*(w)$ on Γ.

The stress resultants at a point inside Ω are given as

$$M_x = -D(w_{,xx} + \nu w_{,yy}), \quad M_y = -D(w_{,yy} + \nu w_{,xx}), \quad M_{xy} = D(1-\nu)w_{,xy} \tag{6a,b,c}$$

$$Q_x = -D\nabla^2 w_{,x} - D_{,x}(w_{,xx} + \nu w_{,yy}) - D_{,y}(1-\nu)w_{,xy}, \tag{6d}$$

$$Q_y = -D\nabla^2 w_{,y} - D_{,y}(w_{,yy} + \nu w_{,xx}) - D_{,x}(1-\nu)w_{,xy}. \tag{6e}$$

3. The AEM as boundary-only method

We solve the boundary-value problem described by Equations (1) and (2) using the AEM. This method is applied to the problem at hand as follows.

Let w be the sought solution of Equation (1). This function is four times continuously differentiable with respect to the spatial co-ordinates x, y in Ω and three times on its boundary Γ. If the biharmonic operator is applied to this function we have

$$\nabla^4 w = b(\mathbf{x}). \tag{7}$$

Equation (7), which henceforth will be referred to as the analog equation of the problem, indicates that the solution of the original boundary-value problem can be obtained as the solution of a linear bending problem for a plate having unit stiffness and subjected to a fictitious load $b = b(\mathbf{x})$ under the given boundary conditions. The unknown load distribution $b = b(\mathbf{x})$ is established using the direct BEM for thin plates with constant thickness (*e.g.* [5], [16, Part 1]) based on the Rayleigh-Green reciprocal identity [17, p. 237] after modifying it to include the natural boundary quantities, *i.e.*, the normal bending moment and the reaction force along the boundary. Although this approach demands the evaluation of hypersingular kernels, it is preferred to the indirect method developed by Katsikadelis and Armenakas [7], because the latter requires the solution of simultaneous boundary differential equations.

The solution of Equation (7) is written in integral form as

$$w(\mathbf{x}) = \int_\Omega \nu b \, \mathrm{d}\Omega + \int_\Gamma [\nu V(w) - w V(\nu) - \nu_{,n} M(w) + w_{,n} M(\nu)] \, \mathrm{d}s + \sum_{l=1}^{L} ([\![\nu T(w) - w T(\nu)]\!])_l, \tag{8}$$

where

$$\nu = \frac{1}{8\pi} r^2 \log r, \qquad r = \|\xi - \mathbf{x}\|, \qquad \mathbf{x} \in \Omega, \xi \in \Gamma \tag{9}$$

is the fundamental solution of the biharmonic equation and

$$V = -[\frac{\partial}{\partial n}\nabla^2 - (\nu - 1)\frac{\partial}{\partial s}(\frac{\partial^2}{\partial n \partial s} - \kappa \frac{\partial}{\partial s})], \tag{10}$$

$$M = M^*/D = -[\nabla^2 + (\nu - 1)(\frac{\partial^2}{\partial s^2} + \kappa \frac{\partial}{\partial n})], \tag{11}$$

$$T = T^*/D = (1 - \nu)(\frac{\partial^2}{\partial s \partial n} - \kappa \frac{\partial}{\partial s}) \tag{12}$$

are the operators that produce the boundary reactions of the fictitious plate, *i.e.*, the effective shear force, the normal bending moment and the twisting moment along the boundary.

The domain integral in Equation (8) can be converted to a line integral on the boundary Γ by means of the dual reciprocity method [18, Chapter 3]. For this reason the fictitious load b is approximated by

$$b = \sum_{j=1}^{M} a_j f_j, \tag{13}$$

where $f_j = f_j(r)$ are M radial-basis approximation functions and a_j are M coefficients to be determined. Note that $r \equiv r_{j\mathbf{x}} = \|\mathbf{x} - \mathbf{x}_j\|$ is the distance between the collocation point $\mathbf{x}_j := \{x_j; y_j\}$ and any point $\mathbf{x} = \{x, y\} \in \Omega \cup \Gamma$ (see Figure 2).

Thus, the domain integral is written as

$$\int_\Omega \nu b \mathrm{d}\Omega = \sum_{j=1}^{M} \left(a_j \int_\Omega \nu f_j \mathrm{d}\Omega \right). \tag{14}$$

If we define the function $\hat{w}_j = \hat{w}_j(r_{j\mathbf{x}}) = \hat{w}_j(\mathbf{x})$ as a particular solution of

$$\nabla^4 \hat{w}_j = f_j \tag{15}$$

and use the Rayleigh-Green identity, we obtain

$$\int_\Omega \nu f_j \mathrm{d}\Omega = \int_\Omega \nu \nabla^4 \hat{w}_j \mathrm{d}\Omega = \int_\Omega \hat{w}_j \nabla^4 \nu \mathrm{d}\Omega + \int_\Gamma \left[\nu (\nabla^2 \hat{w}_j)_{,n} - \hat{w}_j \left(\nabla^2 \nu \right)_{,n} - \nu_{,n} \nabla^2 \hat{w}_j + \hat{w}_{j,n} \nabla^2 \nu \right] \mathrm{d}s. \tag{16}$$

A particular solution of Equation (15) can always be established, if f_j is specified.

Taking into account that

$$\nabla^4 \nu = \delta(\mathbf{y} - \mathbf{x}), \mathbf{y}, \mathbf{x} \in \Omega, \tag{17}$$

we may write Equation (16) as

$$\int_\Omega \nu f_j \mathrm{d}\Omega = \hat{w}_j + \int_\Gamma \left[\nu (\nabla^2 \hat{w}_j)_{,n} - \hat{w}_j (\nabla^2 \nu)_{,n} - \nu_{,n} \nabla^2 \hat{w}_j + \hat{w}_{j,n} \nabla^2 \nu \right] \mathrm{d}s, \tag{18}$$

which is substituted in Equation (8) to yield

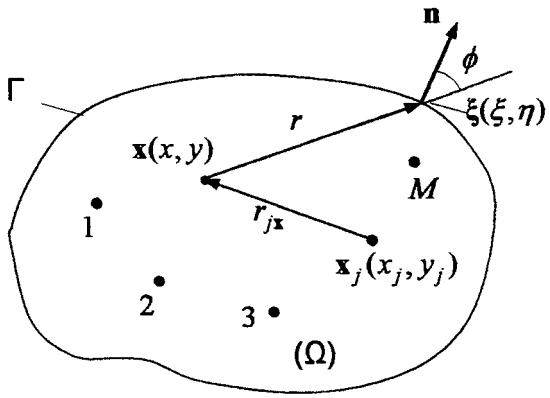

Figure 2. Field point $\mathbf{x}$, source point ξ and collocation point $\mathbf{x}_j$

$$w(\mathbf{x}) = \sum_{j=1}^{M} a_j \left\{ \hat{w}_j(\mathbf{x}) + \int_\Gamma \left[\nu(\nabla^2 \hat{w}_j)_{,n} - \hat{w}_j(\nabla^2 \nu)_{,n} - \nu_{,n} \nabla^2 \hat{w}_j + \hat{w}_{j,n} \nabla^2 \nu \right] \mathrm{d}s \right\} + \int_\Gamma [\nu V(w) - w V(\nu) - \nu_{,n} M(w) + w_{,n} M(\nu)] \mathrm{d}s + \sum_{l=1}^{L} [\![\nu T(w) - w T(\nu)]\!]_l. \tag{19}$$

Letting point $\mathbf{x} \in \Omega$ in Equation (19) coincide with a point $\mathbf{x} \in \Gamma$, we obtain the following integral representations for the deflection and its normal derivative:

$$\frac{\alpha}{2\pi} w(\mathbf{x}) = \sum_{j=1}^{M} a_j \left\{ \frac{\alpha}{2\pi} \hat{w}_j(\mathbf{x}) + \int_\Gamma \left[\nu(\nabla^2 \hat{w}_j)_{,n} - \hat{w}_j(\nabla^2 \nu)_{,n} - \nu_{,n} \nabla^2 \hat{w}_j + \hat{w}_{j,n} \nabla^2 \nu \right] \mathrm{d}s \right\} + \int_\Gamma [\nu V(w) - w V(\nu) - \nu_{,n} M(w) + w_{,n} M(\nu)] \mathrm{d}s + \sum_{l=1}^{L} [\![\nu T(w) - w T(\nu)]\!]_l, \tag{20}$$

$$\alpha_x w_{,x}(\mathbf{x}) + \alpha_y w_{,y}(\mathbf{x}) = \sum_{j=1}^{M} a_j \left\{ \left[\alpha_x \hat{w}_{j,x}(\mathbf{x}) + \alpha_y \hat{w}_{j,y}(\mathbf{x}) \right] + \int_\Gamma \left[\nu_{,v} (\nabla^2 \hat{w}_j)_{,n} - \hat{w}_j(\nabla^2 \nu)_{,nv} - \nu_{,nv} \nabla^2 \hat{w}_j + \hat{w}_{j,n}(\nabla^2 \nu)_{,v} \right] \mathrm{d}s \right\} + \int_\Gamma [\nu_{,v} V(w) - w V(\nu_{,v}) - \nu_{,,v} M(w) + w_{,n} M(\nu_{,v})] \mathrm{d}s + \sum_{l=1}^{L} [\![\nu_{,v} T(w) - w T(\nu_{,v})]\!]_l, \tag{21}$$

where

$$\nu_{,v} = \nu_{,v}(\mathbf{x}, \xi) = \frac{1}{8\pi} r r_{,v} (1 + 2 \log r) \tag{22}$$

is the derivative of the fundamental solution in the direction of the unit vector $\boldsymbol{\nu}(\nu_x, \nu_y)$ at point $\mathbf{x} \in \Gamma$, which coincides with the normal to the boundary at smooth points (see Figure 1). Moreover, $\alpha = \theta_1 - \theta_2$ is the angle between the tangents at point $\mathbf{x} \in \Gamma$ and

$$\alpha_x = \frac{\alpha}{2\pi} \nu_x + \frac{\nu}{2\pi} \left[\frac{1}{2} \nu_x \sin 2\theta + \nu_y \sin^2 \theta \right]_{\theta_1}^{\theta_2}, \tag{23a}$$

$$\alpha_y = \frac{\alpha}{2\pi}\nu_y + \frac{\nu}{2\pi}[\nu_x \sin^2\theta - \frac{1}{2}\nu_y \sin 2\theta]_{\theta_1}^{\theta_2}. \tag{23b}$$

The subscript in ν indicates that the normal derivative is taken with respect to point $\mathbf{x} \in \Gamma$. Since the boundary conditions involve the boundary quantities $M^*(w)$, $V^*(w)$ and $T^*(w)$, a further manipulation is required to express $V(w)$ in terms of the actual effective shear force. Thus, on the base of Equation (3b), we may write

$$V^*(w) = DV(w) + (\nu - 1)D_{,s}\,(w_{,sn} - \kappa w_{,s}) + D_{,n}\,M(w) \tag{24}$$

or

$$V(w) = \frac{1}{D}V^*(w) - (\nu - 1)(\log D)_{,s}\,(w_{,sn} - \kappa w_{,s}) - \frac{1}{D}(\log D)_{,n}\,M^*(w). \tag{25}$$

Further, substituting Equation (25) in Equations (20) and (21), taking into account that $M(w) = M^*(w)/D$, $T(w) = T^*(w)/D$ and performing integration by parts in the terms including $w_{,ns}$ and $w_{,s}$ we have

$$\begin{aligned}\frac{\alpha}{2\pi}w(\mathbf{x}) &= \sum_{j=1}^{M} a_j \left\{\frac{\alpha}{2\pi}\hat{w}_j(\mathbf{x}) + \int_\Gamma \left[\nu(\nabla^2\hat{w}_j)_{,n} - \hat{w}_j(\nabla^2\nu)_{,n} - \nu_{,n}\,\nabla^2\hat{w}_j + \hat{w}_{j,n}\nabla^2\nu\right] \mathrm{d}s\right\} \\ &+ \int_\Gamma \{\Lambda_1(\nu)V^*(w) + \Lambda_2(\nu)w + \Lambda_3(\nu)M^*(w) + \Lambda_4(\nu)w_{,n}\}\mathrm{d}s \\ &+ \sum_{l=1}^{L}\frac{1}{D}[\![\nu T^*(w) - wT^*(\nu)]\!]_l + (\nu - 1)\sum_{l=1}^{L}(\nu(\log D)_{,s}\,[\![\kappa w - w_{,n}]\!])_l,\end{aligned} \tag{26}$$

$$\begin{aligned}&\alpha_x w,x(\mathbf{x}) + \alpha_y w,_y(\mathbf{x}) = \sum_{j=1}^{M} a_j \Big\{[\alpha_x \hat{w}_{j,x}(\mathbf{x}) + \alpha_y \hat{w}_{j,y}(\mathbf{x})] \\ &+ \int_\Gamma [\nu,_v\,(\nabla^2\hat{w}_j)_{,n} - \hat{w}_j(\nabla^2\nu)_{,nv} - v_{,nv}\,\nabla^2\hat{w}_j + \hat{w}_{j,n}(\nabla^2\nu)_{,v}\,\mathrm{d}s\Big\} \\ &+ \int_\Gamma \{\mathrm{K}_1(\nu,_v)V^*(w) + \mathrm{K}_2(\nu,_v)w + \mathrm{K}_3(\nu,_v)M^*(w) + \mathrm{K}_4(\nu,_v)w_{,n}\}\mathrm{d}s \\ &+ \sum_{l=1}^{L}\frac{1}{D}[\![\nu,_v\,T^*(w) - wT^*(\nu,_v)]\!]_l + (\nu - 1)\sum_{l=1}^{L}(\nu,_v\,(\log D)_{,s}\,[\![\kappa w - w_{,n}]\!]_l),\end{aligned} \tag{27}$$

where the new kernels are defined as

$$\Lambda_1(\nu) = \frac{1}{D}\nu, \quad \Lambda_2(\nu) = -V(\nu) - (\nu - 1)[\nu(\log D)_{,s}\,\kappa]_{,s}\,, \tag{28a,b}$$

$$\Lambda_3(\nu) = -\frac{1}{D}[\nu(\log D)_{,n} + \nu_{,n}], \quad \Lambda_4(\nu) = M(\nu) + (\nu - 1)[\nu(\log D)_{,s}]_{,s}\,, \tag{28c,d}$$

$$\mathrm{K}_1(\nu,_v) = \frac{1}{D}\nu,_v\,, \quad \mathrm{K}_2(\nu,_v) = -V(\nu,_v) - (\nu - 1)[\nu,_v\,(\log D)_{,s}\,\kappa]_{,s}\,, \tag{29a,b}$$

$$\mathrm{K}_3(\nu,_v) = -\frac{1}{D}(\nu,_v\,(\log D)_{,n} + \nu_{,nv}], \quad \mathrm{K}_4(\nu,_v) = M(\nu,_v) + (\nu - 1)[\nu,_v\,(\log D)_{,s}]_{,s}\,. \tag{29c,d}$$

For points $\mathbf{x} \in \Gamma$ where the boundary is smooth we have $\alpha = \pi$ and

$$\alpha_x w_{,x}(\mathbf{x}) + \alpha_y w_{,y}(\mathbf{x}) = \frac{1}{2} w_{,v}(\mathbf{x}) \tag{30}$$

and Equations (26) and (27) become

$$\begin{aligned}\frac{1}{2}w(\mathbf{x}) &= \sum_{j=1}^{M} a_j \left\{ \frac{1}{2}\hat{w}_j(\mathbf{x}) + \int_\Gamma [\nu(\nabla^2 \hat{w}_j)_{,n} - \hat{w}_j(\nabla^2\nu)_{,n} - \nu_{,n}\nabla^2\hat{w}_j + \hat{w}_{j,n}\nabla^2\nu]\mathrm{d}s \right\} \\ &+ \int_\Gamma \{\Lambda_1(\nu)V^*(w) + \Lambda_2(\nu)w + \Lambda_3(\nu)M^*(w) + \Lambda_4(\nu)w_{,n}\}\mathrm{d}s \\ &+ \sum_{l=1}^{L} \frac{1}{D}[\![\nu T^*(w) - wT^*(\nu)]\!]_l + (\nu - 1)\sum_{l=1}^{L}(\nu(\log D)_{,s}[\![\kappa w - w_{,n}]\!])_l,\end{aligned} \tag{31}$$

$$\begin{aligned}\frac{1}{2}w(\mathbf{x})_{,v} &= \sum_{j=1}^{M} a_j \left\{ \frac{1}{2}\hat{w}_j(\mathbf{x})_{,v} + \int_\Gamma [\nu_{,v}(\nabla^2\hat{w}_j)_{,n} - \hat{w}_j(\nabla^2\nu)_{,nv} - \nu_{,nv}\nabla^2\hat{w}_j + \hat{w}_{j,n}(\nabla^2\nu)_{,v}]\mathrm{d}s \right\} \\ &+ \int_\Gamma \{\mathrm{K}_1(\nu_{,v})V^*(w) + \mathrm{K}_2(\nu_{,v})w + \mathrm{K}_3(\nu_{,v})M^*(w) + \mathrm{K}_4(\nu_{,v})w_{,n}\}\mathrm{d}s \\ &\sum_{l=1}^{L} \frac{1}{D}[\![\nu_{,v}T^*(w) - wT^*(\nu_{,v})]\!]_l + (\nu - 1\sum_{l=1}^{L}(\nu_{,v}(\log D)_{,s}[\![\kappa w - w_{,n}]\!])_l.\end{aligned} \tag{32}$$

It is worth noting that, if the plate stiffness is constant along the boundary, the terms including $(\log D)_{,s}$ vanish and the kernels are simplified. Moreover, the terms outside the integral are dropped when the boundary is smooth.

At the corner points on the boundary, due to the abrupt change in the orientation of the normal, the normal slope, the bending moment and the equivalent shear force may have discontinuity and a concentrated force may exist. Introducing the double-node concept, we find eight boundary values associated with a corner; two values for the normal slope $[w_{,n}]^{\mp}$, two values of the bending moment $[M^*(w)]^{\mp}$, two values of the effective shear force $[V^*(w)]^{\mp}$, one value of the displacement w, and one value of the concentrated force. Therefore at each corner point eight independent relations are required. One of these is obtained from Equation (26) and two others from Equations (27). The five additional independent relations are furnished by the boundary conditions and the asymptotic smoothness requirement of the solution in the neighborhood of the corner [19]. Guo-Shu and Mukherjee [20] obtained the required additional relations by considering the continuity of the first and second partial derivative with respect to x and y at the corner points. This procedure can be employed also for plates with variable thickness. Some of the more common cases are given in Table 1.

Using N constant elements to approximate the line integrals (see Figure 3) and applying Equations (31) and (32), as well as the boundary conditions (2a,b) at the boundary nodal points, we obtain

$$\begin{bmatrix} \mathbf{A}_{11} & \mathbf{A}_{12} & \mathbf{A}_{13} & \mathbf{A}_{14} \\ \mathbf{A}_{21} & \mathbf{A}_{22} & \mathbf{A}_{23} & \mathbf{A}_{24} \\ \mathbf{A}_{31} & \mathbf{0} & \mathbf{0} & \mathbf{A}_{34} \\ \mathbf{0} & \mathbf{A}_{42} & \mathbf{A}_{43} & \mathbf{0} \end{bmatrix} \begin{Bmatrix} \mathbf{w} \\ \mathbf{w}_n \\ \mathbf{M}^* \\ \mathbf{V}^* \end{Bmatrix} = \begin{bmatrix} \mathbf{B}_{11} \\ \mathbf{B}_{21} \\ \mathbf{0} \\ \mathbf{0} \end{bmatrix} \{\mathbf{a}\} + \begin{Bmatrix} \mathbf{0} \\ \mathbf{0} \\ \boldsymbol{\alpha}_3 \\ \boldsymbol{\beta}_3 \end{Bmatrix}, \tag{33}$$

Table 1. Corner boundary conditions (C=clamped, SS=simply supported, F=free).

Corner support		Relations
(−) side	(+) side	
C	C	$w = 0, [w,_n]^- = [w,_n]^+ = 0, [M^*(w)]^- = [M^*(w)]^+ = 0$
SS	SS	$w = 0, [w,_n]^- = [w,_n]^+ = 0, [M^*(w)]^- = [M^*(w)]^+ = 0,$
F	F	$T^*(w) = 0, [M^*(w)]^- = [M^*(w)]^+ = 0,$
		$[V^*(w)]^- = [V^*(w)]^+ = 0$
C	SS	$w = 0, [w,_n]^- = [w,_n]^+ = 0, [M^*(w)]^- = [M^*(w)]^+ = 0$

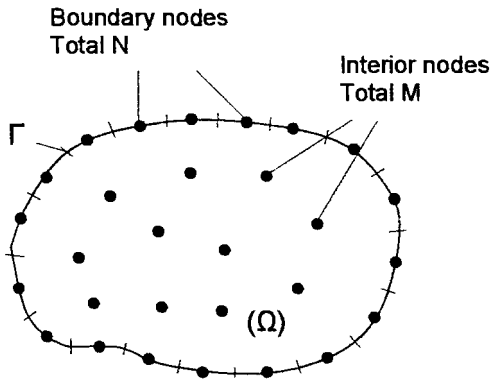

Figure 3. Boundary discretization and domain nodal points

where $\mathbf{A}_{ij}(i = 1, 2)$ are $N \times N$ and $\mathbf{B}_{i1}$ $N \times M$ known matrices originating from the integration of the kernels on the boundary elements and $\mathbf{A}_{ij}(i = 3, 4)$ $N \times N$ diagonal matrices including the nodal values of the functions $\alpha_k = \alpha_k(\mathbf{x})$, $\beta_k = \beta_k(\mathbf{x})$, $(k = 1, 2)$. Finally, $\boldsymbol{\alpha}_3$, $\boldsymbol{\beta}_3$ are $N \times 1$ vectors containing the nodal values of the boundary functions $\alpha_3 = \alpha_3(\mathbf{x})$, $\beta_3 = \beta_3(\mathbf{x})$.

The derivatives of the deflection are obtained by direct differentiation of Equation (19) taking into consideration Equations (28) and (29). Thus, for the shake of conciseness we can write the integral representations of the deflections and its derivatives up to the third order

$$
\begin{aligned}
w(\mathbf{x}),_{pqr} \; = & \sum_{j=1}^{M} a_j \Big\{ \hat{w}_{j,pqr}(\mathbf{x}) + \int_\Gamma \big[\nu,_{pqr} (\nabla^2 \hat{w}_j),_n - \hat{w}_j (\nabla^2 \nu),_{npqr} - \nu,_{npqr} \nabla^2 \hat{w}_j \\
& + \hat{w}_{j,n} \nabla^2 \nu,_{pqr} \big] \mathrm{d}s \Big\} + \int_\Gamma \big\{ \Lambda_1(\nu,_{pqr}) V^*(w) + \Lambda_2(\nu,_{pqr}) w + \Lambda_3(\nu,_{pqr}) M^*(w) \\
& + \Lambda_4(\nu,_{pqr}) w,_n \big\} \mathrm{d}s + \sum_{l=1}^{L} \frac{1}{D} [\![\nu,_{pqr} T^*(w) - w T^*(\nu,_{pqr})]\!]_l \qquad (34) \\
& + (\nu - 1) \sum_{l=1}^{L} (\nu,_{pqr} (\log D),_s [\![\kappa w - w,_n]\!])_l,
\end{aligned}
$$

where $p, q, r = 0, x, y$.

Applying Equation (34) at M points inside Ω, using the same boundary disctretization to approximate the line integrals and noting that for discontinuous elements [21] the corner terms do not contribute, we obtain

$$\mathbf{w}_{,pqr} = \mathbf{A}_{,pqr} + \mathbf{B}_{,pqr}\,\mathbf{w} + \mathbf{C}_{,pqr}\,\mathbf{W_n} + \mathbf{D}_{,pqr}\,\mathbf{M_n^*} + \mathbf{E}_{,pqr}\,\mathbf{V_n^*}, \tag{35}$$

where $\mathbf{A}_{,pqr}$, $\mathbf{B}_{,pqr}$, $\ldots$, $\mathbf{E}_{,pqr}$ are known matrices originating from the integration of the kernels on the boundary elements and $\mathbf{w}_{,pqr}$ the vector of the M values of the designated quantity. It must be emphasized that the kernels in Equations (34) are regular because the distance $r = |\mathbf{x} - \mathbf{y}|$, $\mathbf{x} \in \Omega$, $\mathbf{y} \in \Gamma$ never vanishes during the integration. The integration is performed by Gaussian quadrature. Equations (33) are used to express the boundary quantities in terms of the vector $\mathbf{a}$:

$$\begin{Bmatrix} \mathbf{w} \\ \mathbf{w}_{,n} \\ \mathbf{M}^* \\ \mathbf{V}^* \end{Bmatrix} = \begin{bmatrix} \mathbf{A}_{11} & \mathbf{A}_{12} & \mathbf{A}_{13} & \mathbf{A}_{14} \\ \mathbf{A}_{21} & \mathbf{A}_{22} & \mathbf{A}_{23} & \mathbf{A}_{24} \\ \mathbf{A}_{31} & \mathbf{0} & \mathbf{0} & \mathbf{A}_{34} \\ \mathbf{0} & \mathbf{A}_{42} & \mathbf{A}_{43} & \mathbf{0} \end{bmatrix}^{-1} \left(\begin{bmatrix} \mathbf{B}_{11} \\ \mathbf{B}_{21} \\ \mathbf{0} \\ \mathbf{0} \end{bmatrix} \{\mathbf{a}\} + \begin{Bmatrix} \mathbf{0} \\ \mathbf{0} \\ \boldsymbol{\alpha}_3 \\ \boldsymbol{\beta}_3 \end{Bmatrix} \right), \tag{36}$$

which are subsequently substituted in Equation (35) to yield

$$\mathbf{w}_{,pqr} = \mathbf{H}_{,pqr}\,\mathbf{a} + \mathbf{h}_{,pqr}\,. \tag{37}$$

The matrix $\mathbf{H}_{,pqr}$ has dimensions $M \times M$ and the vector $\mathbf{h}_{,pqr}$ $M \times 1$.

The final step of the AEM is to apply Equation (1) to the M points inside Ω and replace the involved values of the deflection and its derivatives using Equations (37). Thus we obtain the following set of simultaneous nonlinear algebraic equations

$$\mathbf{F}\mathbf{a} + \mathbf{f}(\mathbf{a}) = \mathbf{g}, \tag{38}$$

where $\mathbf{F}$ is a known $M \times M$ matrix, $\mathbf{f}(\mathbf{a})$ a vector of M nonlinear functions of $\mathbf{a}$ and $\mathbf{g}$ the vector of the M values of the load at the interior points. For linear elastic foundation, Equation (38) is further simplified as

$$\overline{\mathbf{F}}\mathbf{a} = \mathbf{g}, \tag{39}$$

where $\mathbf{F}$ is a known $M \times M$ matrix.

Equation (38) or (39) are solved to establish the vector $\mathbf{a}$. Then the values of the deflection and its derivatives are determined from Equation (37). The obtained values are used in Equations (6) to evaluate the stress resultants. The boundary quantities are established from Equation (36) and the subgrade reaction from $p(w, \nabla^2 w)$. For points $\mathbf{x}$ not coinciding with the domain points the respective quantities can be established from the discretized counterparts of Equation (37).

The theoretical background of the AEM is simple, it is explained in [13] and is fully understood from its successful application to solve a large variety of engineering problems described by ordinary and partial differential equations [22]. According to the concept of the analog equation, the reduction of Equation (1) to the substitute equation (7) is not unique. Any fourth-order differential operator may be used to derive the analog equation. However, for the implementation of the method the operator should be the simplest one having a simple known fundamental solution and, thus, a known integral representation of the solution. Apparently, for the problem at hand, the biharmonic operator satisfies these requirements. Nevertheless, the method is still open to a rigorous mathematical foundation, especially when applied to the solution of problems described by parabolic and hyperbolic differential equations. Regarding its application to nonlinear problems, the selection of a linear analog equation does not spoil

the method, since the nonlinearity is transferred to the system of the nonlinear algebraic equations, *i.e.*, Equation (38).

4. Numerical examples

On the basis of the procedure described in the previous section a FORTRAN program has been written for the analysis of plates with variable thickness resting on a nonlinear elastic foundation. Without excluding more general subgrade models, the one adopted herein is the biparametric model

$$p = k_0 w - k_1 w^2 - G\nabla^2 w, \tag{40}$$

where k_0, k_1 and G are given constants. Actually, this model is *triparametric*. Nevertheless, we maintain the term *biparametric*, because it consists of separated nonlinear Winkler's springs ($p = k_0 w - k_1 w^2$), which are enforced to interact by the shear layer with modulus G. Extended literature on subgrade models can be found in Selvadurai [23, Chapter 2].

The approximation functions f_j employed herein are the multiquadrics [24], which are global and defined as

$$f_j = \sqrt{r^2 + c^2}, \tag{41}$$

where c is an arbitrary constant and

$$r = \sqrt{(x - x_j)^2 + (y - y_j)^2} \qquad j = 1, 2, \ldots, M \tag{42}$$

with x_j, y_j being the collocation point. Using these radial-base functions, we obtain the particular solution of Equation (15) as

$$\begin{aligned}\hat{w}_j = &-\frac{1}{12}\log(c\sqrt{r^2 + c^2} + c^2)c^3(r^2 + c^2) + \frac{7}{60}c^5\log(c\sqrt{r^2 + c^2} + c^2) - \frac{1}{12}c^5 + \frac{1}{12}c^3 r^2 \\ &-\frac{7}{60}c^4\sqrt{r^2 + c^2} + \frac{1}{225}(r^2 + c^2)^{5/2} + \frac{2}{45}c^2(r^2 + c^2)^{3/2}.\end{aligned} \tag{43}$$

The selection of the shape parameter c is very important for the accuracy and convergence of the method. There are empirical formulae [25] which might be used to estimate its value. In our examples, values of c ranging between 0·20 and 1·00 give very good results. The optimum value has been tested by comparing the results with those from existing solutions. In cases, however, where no results are available to compare with, the optimum value of c is taken as that minimizing the total potential of the plate. This is shown in Figure 6, where the dependence of the total potential on the shape parameter c is presented for various values of the ratio $\eta = h_0/h_B$ of the plate in Example 3.

The derivatives of $\hat{w}_j$ involved in Equation (34) are obtained using a symbolic language and are converted directly to FORTRAN code. They are not quoted here, because their expressions are too lengthy.

For the presentation of the numerical results the following dimensionless parameters are introduced

$$s = a/\sqrt{D_0/G}, \quad \lambda_i = a/\sqrt[4]{D_0/k_i}, \quad (i = 0, 1), \tag{44}$$

Table 2. Deflections $\overline{w} = w/(g_0 a^4/D_M)$ and bending moments $\bar{M}_x = M_x/g_0 a^2$ at the center of a rectangular clamped plate with linearly varying thickness ($\nu = 0{\cdot}3$).

b/a	λ_0, λ_1, s		h_a/h_0			
			Ref. [26]	Present solution		
			1·0	1·0	1·001	1·2
1·5	$\lambda_0 = 0{\cdot}134$	$\bar{w}$	$0{\cdot}109 \times 10^{-2}$	$0{\cdot}107 \times 10^{-2}$	$0{\cdot}107 \times 10^{-2}$	$0{\cdot}535 \times 10^{-3}$
	$\lambda_1 = 0$					
	$s = 0$	$\bar{M}_x$	$0{\cdot}183 \times 10^{-1}$	$0{\cdot}181 \times 10^{-1}$	$0{\cdot}181 \times 10^{-1}$	$0{\cdot}093 \times 10^{-1}$
	$\lambda_0 = 0{\cdot}134$	$\bar{w}$		$0{\cdot}107 \times 10^{-2}$	$0{\cdot}107 \times 10^{-2}$	$0{\cdot}535 \times 10^{-3}$
	$\lambda_1 = 0{\cdot}01$					
	$s = 0{\cdot}001$	$\bar{M}_x$		$0{\cdot}181 \times 10{-}1$	$0{\cdot}181 \times 10^{-1}$	$0{\cdot}093 \times 10^{-1}$
	$\lambda_0 = 5$	$\bar{w}$		$0{\cdot}342 \times 10^{-3}$	$0{\cdot}343 \times 10^{-3}$	$0{\cdot}483 \times 10^{-3}$
	$\lambda_1 = 0{\cdot}2$					
	$s = 7$	$\bar{M}_x$		$4{\cdot}468 \times 10^{-3}$	$4{\cdot}476 \times 10^{-3}$	$6{\cdot}667 \times 10^{-3}$
1·0	$\lambda_0 = 0{\cdot}134$	$\bar{w}$	$0{\cdot}630 \times 10^{-3}$	$0{\cdot}616 \times 10^{-3}$	$0{\cdot}614 \times 10^{-3}$	$0{\cdot}471 \times 10^{-3}$
	$\lambda_1 = 0$					
	$s = 0$	$\bar{M}_x$	$0{\cdot}114 \times 10^{-1}$	$0{\cdot}113 \times 10^{-1}$	$0{\cdot}113 \times 10^{-1}$	$0{\cdot}089 \times 10^{-1}$
	$\lambda_0 = 0{\cdot}134$	$\bar{w}$		$0{\cdot}616 \times 10^{-3}$	$0{\cdot}614 \times 10^{-3}$	$0{\cdot}471 \times 10^{-3}$
	$\lambda_1 = 0{\cdot}01$					
	$s = 0{\cdot}001$	$\bar{M}_x$		$0{\cdot}113 \times 10^{-1}$	$0{\cdot}113 \times 10^{-1}$	$0{\cdot}089 \times 10^{-1}$
	$\lambda_0 = 5$	$\bar{w}$		$0{\cdot}250 \times 10^{-3}$	$0{\cdot}250 \times 10^{-3}$	$0{\cdot}295 \times 10^{-3}$
	$\lambda_1 = 0{\cdot}2$					
	$s = 7$	$\bar{M}_x$		$3{\cdot}708 \times 10^{-3}$	$3{\cdot}713 \times 10^{-3}$	$4{\cdot}694 \times 10^{-3}$

where a is a characteristic length of the plate (*e.g.*, the length of one side of a rectangular plate) and D_0 its flexural stiffness at the origin of the coordinates. For usual engineering applications it may be $0 \leq s \leq 30$ and $0 \leq \lambda_0 \leq 20$ [26].

4.1. Example 1. Clamped rectangular plate with linearly varying thickness

A clamped rectangular plate $a \times b$ $0 \leq x \leq a$, $0 \leq y \leq b$ with linearly varying thickness $h = h_0(1 + \beta_x x/a)$, $\beta_x = h_a/h_0 - 1$ resting on a biparametric elastic foundation has been studied; h_0 and h_a denote the plate thickness at $x = 0$ and $x = a$. The plate is subjected to the hydrostatic load $g_0 x/a$. The computed deflections $\bar{w} = w/(g_0 a^4/D_M)$, $D_M = Eh_M^3/12(1 - \nu^2)$, $h_M = (h_0 + h_a)/2$ and bending moments $\bar{M}_x = M_x/g_0 a^2$ are presented in Table 2. The numerical results have been obtained using $N = 80$ and $M = 81$ nodal points. Note that as anticipated the deflections approach those given in [26] for a plate with constant thickness when $h_a/h_0 \to 1$, $\lambda_1 \to 0$, $s \to 0$.

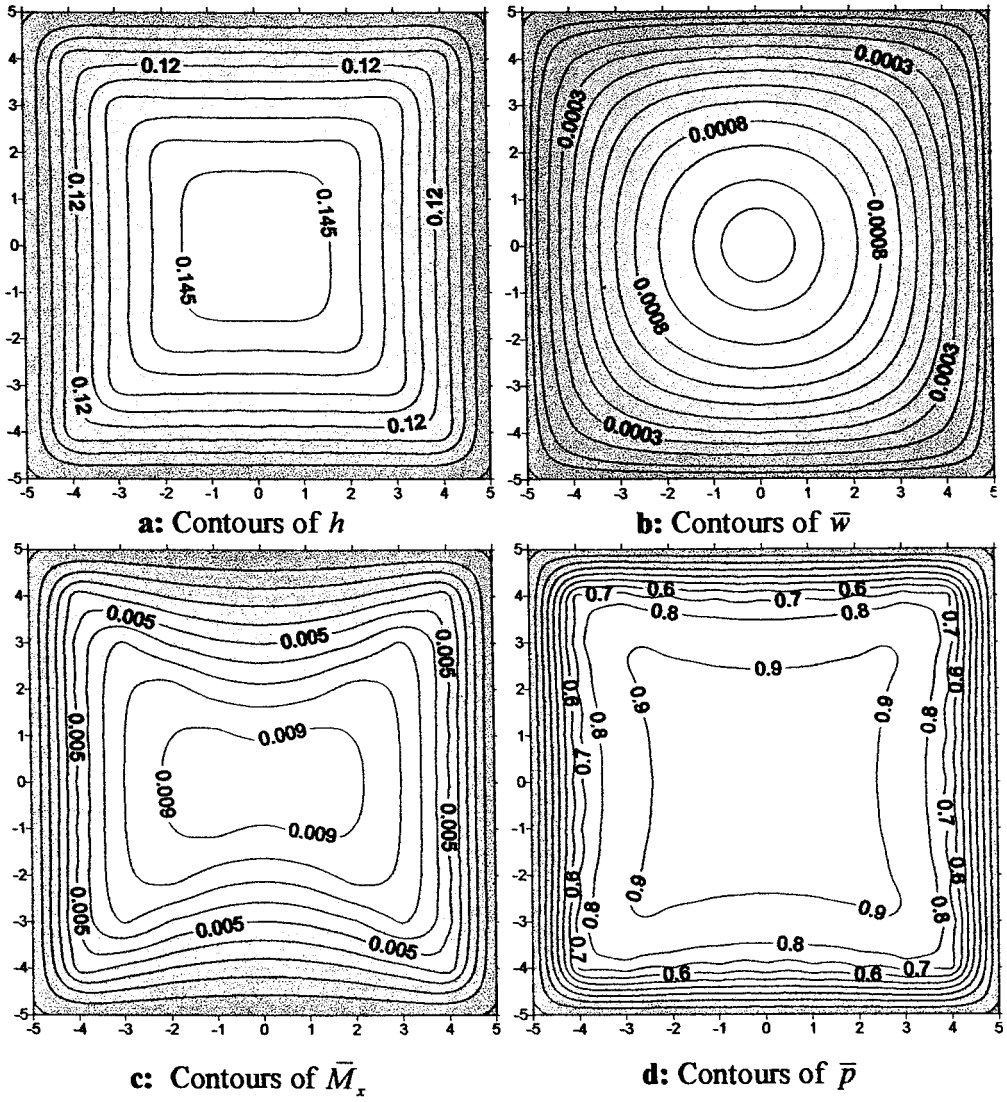

Figure 4. Simply supported square plate with quadratic thickness variation.

4.2. EXAMPLE 2. SIMPLY SUPPORTED SQUARE PLATE WITH LINEARLY VARYING THICKNESS

A simply supported square plate $0 \leq x \leq a$, $0 \leq y \leq b$ with linearly varying thickness $h = h_0(1 + \beta_x x/a)$, $\beta_x = h_a/h_0 - 1$ resting on a biparametric elastic foundation has been studied; h_0 and h_a are the plate thicknesses at $x = 0$ and $x = a$. The plate is subjected to uniform load $g = g_0$. The computed deflections $\bar{w} = w/(g_0 a^4/D_M)$, $D_M = Eh_M^3/12(1-\nu^2)$, $h_M = (h_0 + h_a)/2$ and bending moments $\bar{M}_x = M_x/g_0 a^2$ are presented in Table 3. The numerical results have been obtained using $N = 80$ and $M = 81$ nodal points. Note that the deflections approach those given in [8] for the plate with constant thickness resting on linear Winkler's foundation, when $h_a/h_0 \to 1$ and $\lambda_1 \to 0$ $s \to 0$.

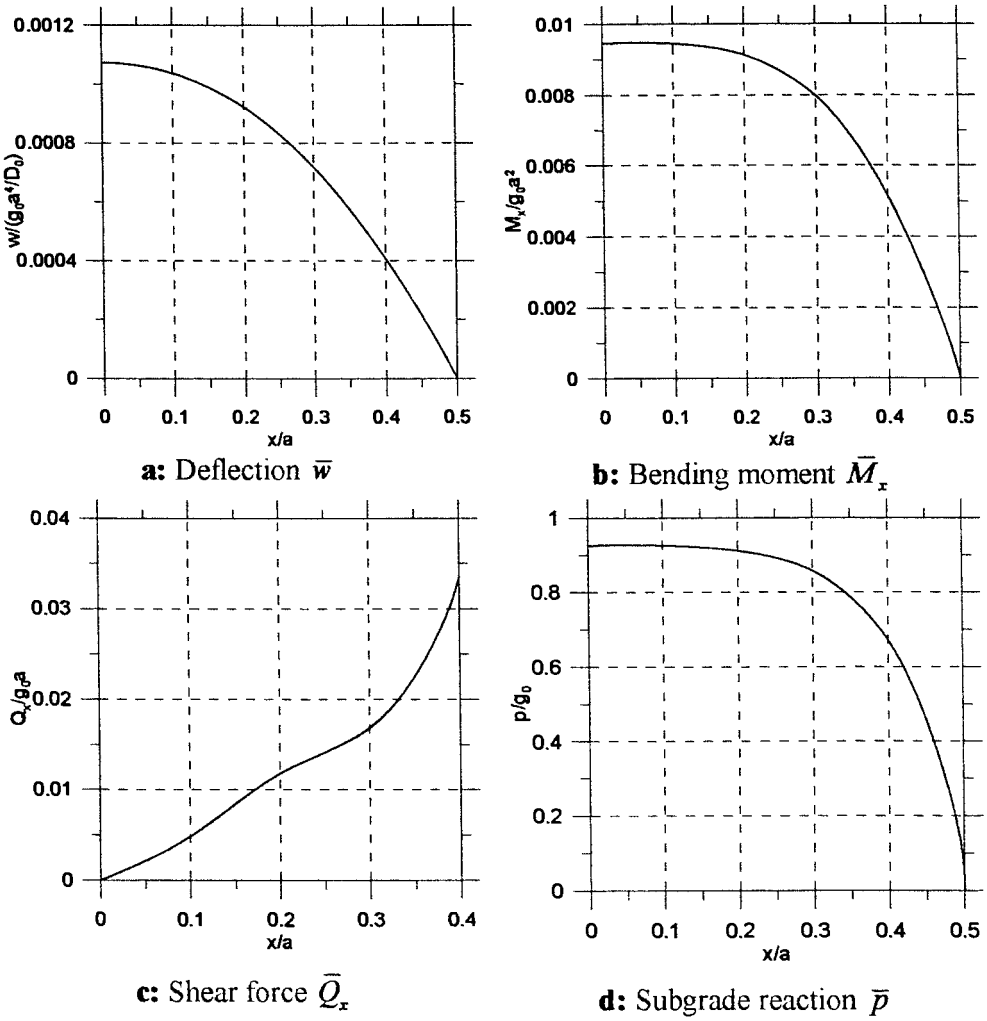

Figure 5. Variation of $\bar{w} = w/(g_0 a^4/D_0)$, $\bar{M}_x = M_x/g_0 a^2$, $\bar{Q}_x = Q_x/g_0 a$ and $\bar{p} = p/g_0$ along the the x-axis in the plate of Example 3.

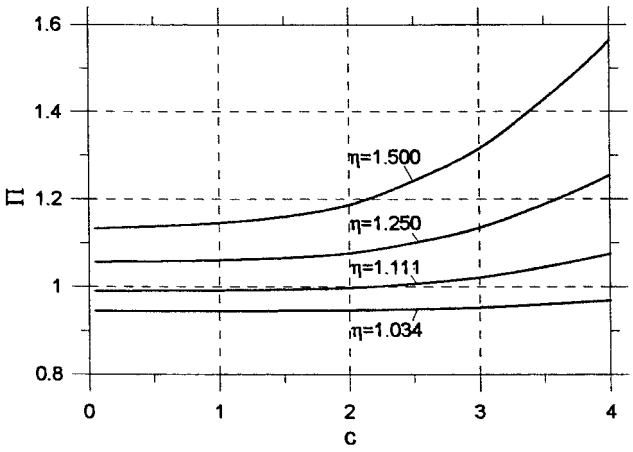

Figure 6. Dependence of total potential $\Pi(c)$ on the shape parameter c.

Table 3. Deflections $\bar{w} = w/(g_0 a^4/D_M)$ and bending moments $\bar{M}_x = M_x/g_0 a^2$ at the center of a square simply supported plate with linearly varying thickness ($\nu = 0{\cdot}3$).

b/a	λ_0, λ_1, s		h_a/h_0			
			Ref. [8]	Present solution		
			1·0	1·0	1·001	1·2
1·0	$\lambda_1 = 3{\cdot}76$	$\bar{w}$	$0{\cdot}2671 \times 10^{-2}$	$0{\cdot}2653 \times 10^{-2}$	$0{\cdot}2654 \times 10^{-2}$	$0{\cdot}3706 \times 10^{-2}$
	$\lambda_1 = 0$					
	$s = 0$	$\bar{M}_x$	0·0301	0·0299	0·0299	0·0420
	$\lambda_0 = 3{\cdot}76$	$\bar{w}$		$0{\cdot}2653 \times 10^{-2}$	$0{\cdot}2654 \times 10^{-2}$	$0{\cdot}3706 \times 10^{-2}$
	$\lambda_1 = 0{\cdot}01$					
	$s = 0{\cdot}001$	$\bar{M}_x$		0·0299	0·0299	0·0420
	$\lambda_0 = 5$	$\bar{w}$		$0{\cdot}7554 \times 10^{-3}$	$0{\cdot}7564 \times 10^{-3}$	$1{\cdot}1533 \times 10^{-3}$
	$\lambda_1 = 0{\cdot}2$					
	$s = 7$	$\bar{M}_x$		$0{\cdot}721 \times 10^{-4}$	$0{\cdot}722 \times 10^{-4}$	0·0143

Table 4. Deflections $\bar{w} = w/(g_0 b^4/D_0)$ and bending moments $\bar{M}_x = M_x/g_0 b^2$ at the center of an elliptic simply supported plate with quadratic thickness variation ($\nu = 0{\cdot}3$).

			h_0/h_B		
a/b	λ_0, λ_1, s		1·0	1·2	1·5
1	$\lambda_0 = 2{\cdot}11$	$\bar{w}$	$0{\cdot}4384 \times 10^{-2}$	$0{\cdot}4427 \times 10^{-2}$	$0{\cdot}4455 \times 10^{-2}$
	$\lambda_1 = 3$	$\bar{M}_x$	$0{\cdot}1225 \times 10^{-1}$	$0{\cdot}1206 \times 10^{-1}$	$0{\cdot}1188 \times 10^{-1}$
	$s = 7$	$\bar{p}$	0·9979	0·9844	0·9709
7·5/5	$\lambda_0 = 2{\cdot}11$	$\bar{w}$	$0{\cdot}1327 \times 10^{-1}$	$0{\cdot}1359 \times 10^{-1}$	$0{\cdot}1383 \times 10^{-1}$
	$\lambda_1 = 3$	$\bar{M}_x$	$0{\cdot}2211 \times 10^{-1}$	$0{\cdot}2028 \times 10^{-1}$	$0{\cdot}1855 \times 10^{-1}$
	$s = 7$	$\bar{p}$	0·9774	0·9576	0·9371

4.3. Example 3. Simply supported square plate with quadratic thickness variation law

A simply supported square plate with side length a has been analyzed. The thickness variation law is specified by the function $h(r) = (h_B - h_0)(r/R)^2 + h_0$, $0 \le r \le R$, where h_0 is the plate thickness at the center of the plate and h_B its constant thickness along the boundary; R is the radial distance from the center of the plate to the boundary. The contours of the plate thickness are shown in Figure 4a. The plate is subjected to uniform load $g = g_0$. The numerical results have been obtained for $a = 10$ m, $E = 2{\cdot}1 \times 10^6$ kN/m^2, $\nu = 0{\cdot}3$, $\lambda_0 = 3{\cdot}76$, $\lambda_1 = 3{\cdot}16$, $s = 7$, $h_0 = 0{\cdot}15$ m, $h_B = 0{\cdot}10$ m, $N = 80$, $M = 81$. The contours of the computed deflection $\bar{w} = w/(g_0 a^4/D_0)$, bending moment $\bar{M}_x = Mx/g_0 a^2$ and subgrade reaction $\bar{p} = p/g_0$ are shown in Figures 4b, c, d. Moreover, in Figure 5 the variation of $\bar{w} = w/(g_0 a^4/D_0)$,

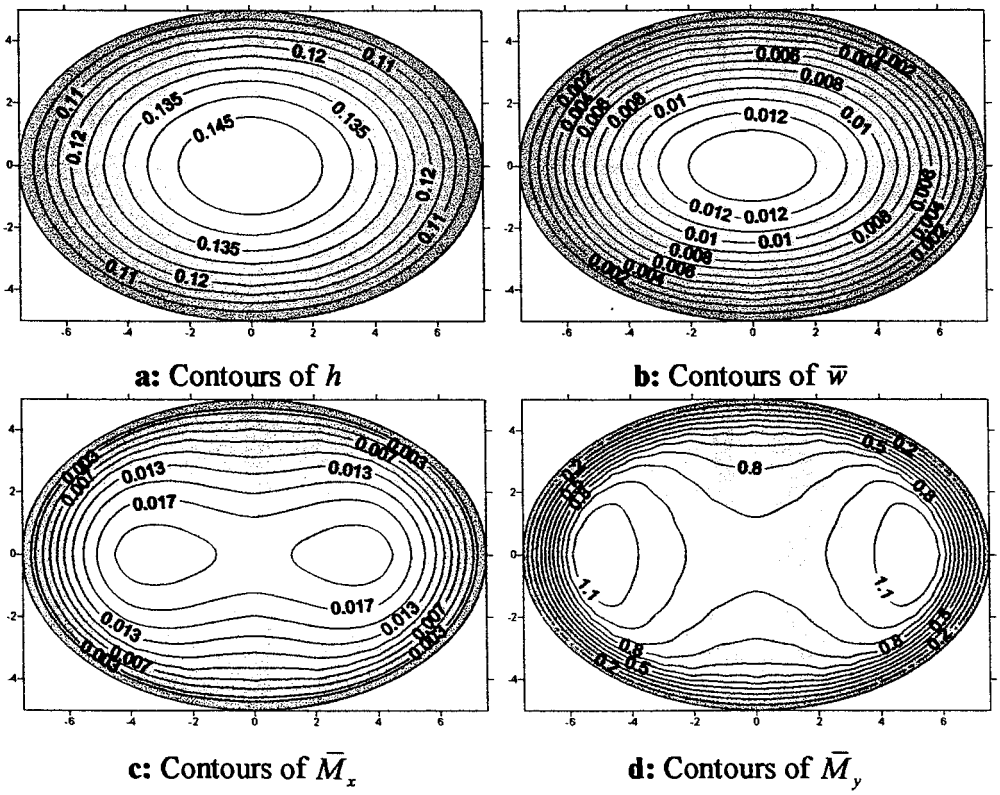

Figure 7. Simply supported elliptic plate with quadratic thickness variation.

$\bar{M}_x = M_x/g_0a^2$, $\bar{Q}_x = Q_x/g_0a$ and $\bar{p} = p/g_0$ along the x-axis are presented. Finally, the dependence of total potential $\Pi(x)$ of the plate on the shape parameter c is shown for various values of $\eta = h_0/h_B$, which permits the selection of an optimum value of c.

4.4. Example 4. Elliptic simply supported plate with quadratic thickness variation law

A simply supported elliptic plate resting on a nonlinear biparametric foundation has been analyzed. Its boundary is defined by the ellipse $x = a\ \cos\theta$, $y = b\ \sin\theta$, $0 \le \theta \le 2\pi$. The thickness-variation law is specified by the function $h(r) = (h_B - h_0)(r/R)^2 + h_0$, $0 \le r \le R$, where h_0 is the plate thickness at the center of the plate and h_B its constant thickness along the boundary; $R = \sqrt{x^2 + y^2}$ is the radial distance from the center of the plate to the boundary. The contours of the plate thickness are shown in Figure 7a. The curvature of the elliptic boundary is obtained as $\kappa(s) = ab/[a^2 + (b^2 - a^2)\cos\theta^2]^{3/2}$. The plate is subjected to uniform load $g = g_0$. The numerical results have been obtained for $E = 2{\cdot}1 \times 10^6$ kN/m^2, $\nu = 0{\cdot}3$, $\lambda_0 = 2{\cdot}11$, $\lambda_1 = 3$, $s = 7$, $h_0 = 0{\cdot}15$ m, $h_B = 0{\cdot}10$ m, $N = 80$, $M = 81$. The computed deflections $\bar{w} = w/(g_0b^4/D_0)$, bending moments $\bar{M}_x = M_x/g_0b^2$ and the subgrade reaction $\bar{p} = p/g_0$ are presented in Table 4. Moreover, the contours of the computed deflections $\bar{w} = w/(g_0b^4/D_0)$, bending moments $\bar{M}_x = M_x/g_0b^2$ and $\bar{M}_y = M_y/g_0b^2$ are shown in Figures 7b–d.

5. Conclusions

In this paper the BEM has been developed for the analysis of plates with variable stiffness resting on a nonlinear biparametric foundation. The presented method is based on the concept of the analog equation, which replaces the original problem to that of a plate with constant thickness not resting on a foundation. From the presented analysis and the numerical examples the following main conclusions can be drawn:

As the method is boundary-only, it has all the advantages of the pure BEM, *i.e.*, the discretization and integration are performed only on the boundary.

The known fundamental solution of the biharmonic equation is employed to derive the integral representation of the solution, and therefore the inability to establish the fundamental solution of the governing equation is overcome.

The deflection, the stress resultants and the subgrade reaction at any point are computed using the respective integral representations as mathematical formulae.

Accurate numerical results for the displacements and the stress resultants are obtained using multiquadrics.

The concept of the analog equation in conjunction with radial-basis-functions approximation of the fictitious sources renders the BEM a versatile computational method for solving difficult nonlinear engineering problems.

References

1. M. S. Nerantzaki, Analysis of plates with variable thickness by the analog equation method. In: C.A. Brebbia, S. Kim, T. A. Osswald and H. Power (eds.), *Boundary Elements XVII*. Southampton: Computational Mechanics Publications (1995) 175–184.
2. M. S. Nerantzaki and J. T. Katsikadelis, Vibrations of plates with variable thickness: An analog equation solution. In: G. Augusti, C. Borri and P. Spinelli (eds.), *Structural Dynamics, Eurodyn '96*. Rotterdam: Balkema Publishers (1996) 711–717.
3. M. S. Nerantzaki and J. T. Katsikadelis, An analog equation solution to dynamic analysis of plates with variable thickness. *Engng. Anal. Bound. Elem.* 17 (1996) 145–152.
4. M. S. Nerantzaki and J. T. Katsikadelis, Buckling of plates with variable thickness- An analog equation solution. *Engng. Anal. Bound. Elem.* 18 (1996) 149–154.
5. M. Stern, A general boundary integral formulation for the numerical solution of plate bending problems. *Int. J. Solids Struct.* 15 (1979) 769–782.
6. F. Hartmann and R. Zotemantel, The direct boundary element method in plate bending. *Int. J. Num. Methods Engnng.* 23 (1986) 2049–2069.
7. J. T. Katsikadelis and A. E. Armenakas, A new boundary equation solution to the plate problem. *ASME J. Appl. Mech.* 56 (1989) 364–374.
8. F. Paris and S. de Leon, Thin plates by the boundary element method by means of two Poissons equations. *Engng. Anal. Bound. Elem.* 17 (1996) 111–122.
9. D. Beskos (ed.), *Boundary Element Analysis of Plates and Shells*. Berlin: Springer-Verlag (1991) 368 pp.
10. E. J. Sapountzakis and J. T. Katsikadelis, Boundary element solution for plates of variable thickness. *ASCE J. Engng. Mech.* 117 (1991) 1241–1256.
11. J. T. Katsikadelis and E. J. Sapountzakis, A BEM solution to dynamic analysis of plates with variable thickness. *Comp. Mech.* 7 (1991) 369–379.
12. E. W. V. Chaves, G. R. Fernandes and W. S. Venturini, Plate bending boundary element formulation considering variable thickness. *Engng. Anal. Bound. Elem.* 23 (1999) 405–418.
13. J. T. Katsikadelis, The analog equation method-A powerful BEM-based solution technique for solving linear and nonlinear engineering problems. In: C. A. Brebbia (ed.), *Boundary Element Method XVI*, Southampton: Computational Mechanics Publications (1994) 167–182.

14. S. P. Timoshenko and S. Woinowsky-Krieger, *Theory of Plates and Shells*. (2nd ed.). New York: McGraw-Hill (1959) 580 pp.
15. J. T. Katsikadelis and L. F. Kallivokas, Plates on biparametric elastic foundation by BDIE method. *J. Engng. Mech.* 114, (1988) 847–875.
16. J. T. Katsikadelis, *The Analysis of Plates on Elastic Foundation by the Boundary Integral Equation Method*. (Dissertation for the degree of Doctor of Philosophy) New York: Polytechnic University of New York (1982) 293 pp.
17. S. Bergmann and M. Schiffer, *Kernel Functions and Elliptic Differential Equations in Mathematical Physics*. New York: Academic Press (1953) 432 pp.
18. P. W. Partridge, C. A. Brebbia and L. D. Wrobel, *The Dual Reciprocity Boundary Element Method*. Southampon Computational Mechanics Publications, London Elsevier Applied Science (1991) 276 pp.
19. M. L. Williams, Surface stress singularities resulting from various boundary conditions in angular corners of plate under bending. In: *Proc. First U.S. Nat. Congress of Applied Mechanics*, ASME (1952) pp. 325–329.
20. S. Guo-Shu and S. Mukherjee, Boundary element method analysis of bending of elastic plates of arbitrary shape with general boundary conditions. *Engng. Anal. Bound. Elem.* 3 (1986) 36–44.
21. W. S. Venturini and J. B. Paiva, Boundary element for plate bending analysis. *Engng. Anal. Bound. Elem.* 11 (1993) 1–8.
22. J. T. Katsikadelis, The analog boundary integral equation method for nonlinear static and dynamic problem in continuum mechanics. *J. Theor. Appl. Mech.* 40 (2002) 961–984.
23. A. P. S. Selvadurai, *Elastic Analysis of Soil-Foundation Interaction*. Amsterdam: Elsevier (1979) 543 pp.
24. M. A. Goldberg, C. S. Chen and S. P. Karur, Improved multiquadric approximation for partial differential equations. *Engng. Anal. Bound. Elem.* 18 (1996) 9–17.
25. R. E. Carlson and T. A. Foley, The parameter R^2 in multiquadric interpolation. *Computers Math. Applic.* 21 (9) (1991) 29–42.
26. J. T. Katsikadelis and L. F. Kallivokas, Clamped plates on Pasternak-type elastic foundation by the boundary element method. *ASME J. Appl. Mech.* 53 (1986) 909–917.